

Chaotic Dynamics in Multi-LLM Deliberation

Hajime Shimao^{1,*}, Warut Khern-am-nuai², and Sung Joo Kim³

¹The Pennsylvania State University, Malvern, PA, USA

²McGill University, Montreal, QC, Canada

³American University, Washington, DC, USA

*Corresponding author: hjs5825@psu.edu

Abstract

Collective AI systems increasingly rely on multi-LLM deliberation, but their stability under repeated execution remains poorly characterized. We model five-agent LLM committees as random dynamical systems and quantify inter-run sensitivity using an empirical Lyapunov exponent ($\hat{\lambda}$) derived from trajectory divergence in committee mean preferences. Across 12 policy scenarios, a factorial design at $T = 0$ identifies two independent routes to instability: role differentiation in homogeneous committees and model heterogeneity in no-role committees. Critically, these effects appear even in the $T = 0$ regime where practitioners often expect deterministic behavior. In the HL-01 benchmark, both routes produce elevated divergence ($\hat{\lambda} = 0.0541$ and 0.0947 , respectively), while homogeneous no-role committees also remain in a positive-divergence regime ($\hat{\lambda} = 0.0221$). The combined mixed+roles condition is less unstable than mixed+no-role ($\hat{\lambda} = 0.0519$ vs. 0.0947), showing non-additive interaction. Mechanistically, Chair-role ablation reduces $\hat{\lambda}$ most strongly, and targeted protocol variants that shorten memory windows further attenuate divergence. These results support stability auditing as a core design requirement for multi-LLM governance systems.

Introduction

Large language models are rapidly moving from single-agent usage to committee-like deployments in which multiple agents exchange arguments and then vote or synthesize a decision [Wu et al., 2023, Chen et al., 2023, Li et al., 2023, Hong et al., 2023, Park et al., 2023]. For these systems, reproducibility is a governance property, not only an engineering convenience [Gundersen and Kjensmo, 2018, Pineau et al., 2021]. If nominally identical committee runs diverge into different trajectories and final decisions, institutions face uncertainty that standard one-shot model evaluation does not capture. This concern is strongest at $T = 0$: if instability persists when explicit sampling noise is minimized, unpredictability is structural rather than a temperature artifact.

Prior work has established instability of prompt-level LLM

outputs [Sclar et al., 2024, Zheng et al., 2023], and social-science literature shows that group outcomes are sensitive to composition and framing [Sunstein, 2002, Tversky and Kahneman, 1981, Page, 2007]. Recent agent-safety work also uses “chaos” in a broader descriptive sense for deployment failures in autonomous systems [Shapira et al., 2026]; our use is narrower and dynamical: trajectory-sensitive divergence quantified by an empirical Lyapunov-style estimand. What is missing is an experimentally identified design map for *multi-LLM* instability: which architectural choices create, amplify, or attenuate divergence in collective AI deliberation.

We study this as a random dynamical system [Arnold, 1998]. The core experiment crosses two design axes: role structure (NOROLES vs. ROLES) and model composition (uniform provider/model vs. heterogeneous mixed committee). We then test mechanism (role ablation), intervention (reduced memory depth), and a direct falsification target (near-memoryless update). The central empirical claim is that instability is design-induced and experimentally decomposable into two routes with non-additive interaction. The key practical implication is that unpredictability can remain material even under seemingly “deterministic” settings.

Results

In plain terms, we find that the same AI committee can reach different collective trajectories and decisions even when run repeatedly under nominally identical settings, including at $T = 0$. Two design choices most strongly shape this instability: assigning differentiated institutional roles, and mixing different model families within one committee. Across experiments, these factors do not combine additively, and targeted protocol changes can reduce instability. The results below quantify these effects, identify a key amplification mechanism, and test intervention/falsification predictions.

Experimental design and estimand

Each run executes a five-agent committee for 20 rounds. At each turn, each agent outputs an argument and structured

preference state $\mathbf{s}_t^{(i)} = (p_A, p_B, p_C, \text{conf})$. For replicate r , we compute the committee mean trajectory $\bar{\mathbf{p}}_t^{(r)} = \frac{1}{N} \sum_i \mathbf{s}_t^{(i)}$ on the simplex. Inter-replicate divergence is

$$D(t) = \frac{2}{R(R-1)} \sum_{i < j} \left\| \bar{\mathbf{p}}_t^{(i)} - \bar{\mathbf{p}}_t^{(j)} \right\|_2. \quad (1)$$

We estimate $\hat{\lambda}$ as the slope of $\log D(t)$ over rounds 3–20. Positive $\hat{\lambda}$ indicates exponential divergence of trajectories. Unless otherwise noted, target replicate count is $R = 20$ per condition.

Two design routes and non-additive interaction

Figure 1A shows HL-01 trajectories under three canonical conditions at $T = 0$. Homogeneous NOROLES is lower-divergence but still positive ($\hat{\lambda} = 0.0221$), while adding role mandates in a homogeneous committee increases divergence ($\hat{\lambda} = 0.0541$). Independently, heterogeneous model composition without roles also yields high divergence ($\hat{\lambda} = 0.0947$). These correspond to two distinct routes to stronger instability: institutional differentiation (Route A) and compositional heterogeneity (Route B), both amplifying a non-zero baseline.

Figure 1B provides the full HL-01 2×2 matrix. The mixed+roles cell is substantially less unstable than mixed+no-role ($\hat{\lambda} = 0.0519$ vs. 0.0947), indicating non-additivity. Thus, increasing both diversity dimensions does not monotonically increase instability [Hong and Page, 2004, Page, 2007].

Figure 4 extends this to the 12-scenario benchmark at $T = 0$. Across scenarios, uniform NOROLES is generally the lowest-divergence configuration, but often still shows $\hat{\lambda} > 0$. Uniform ROLES and mixed NOROLES are frequently more elevated. The mixed ROLES condition remains heterogeneous in magnitude but is fully estimated across the scenario set (realized $n = 20$ per mixed cell). This closes the previously incomplete mixed-model matrix and shifts the claim from single-scenario demonstration to benchmark-level pattern.

Mechanism: Chair role as dominant amplifier

Figure 2 isolates the Chair channel in a canonical single-scenario mechanism panel. In HL-01 (panel A), role-ablation effects are reported on the same $\Delta\hat{\lambda} = \hat{\lambda}_{\text{full roles}} - \hat{\lambda}_{\text{ablated}}$ scale used in panel B, showing the largest reduction for Chair ablation; other single-role ablations are near zero or negative in this scenario. Panel B shows cross-scenario heterogeneity in this effect using $\Delta\hat{\lambda} = \hat{\lambda}_{\text{full roles}} - \hat{\lambda}_{\text{ablate Chair}}$ across five scenarios (IM-01, HL-01, CL-01, SP-03, AI-01). All five point estimates are positive, but uncertainty differs by scenario: 95% CIs exclude zero in IM-01 and HL-01, while the remaining three are directionally positive but inconclusive at current sample size. This pattern supports a mechanistic interpretation in which synthesis-focused Chair behavior is an important, scenario-contingent amplification channel [Kerr and Tindale, 2004].

Intervention and falsification tests

Figure 3 reports two protocol stress tests. First, reducing argument-memory depth from $k = 15$ to $k = 3$ (intervention) lowers $\hat{\lambda}$ in all four tested scenarios (AI-01, CL-01, HL-01, SP-03). Second, a stricter memory-collapse variant ($k = 1$) in IM-01 and CL-01 lowers $\hat{\lambda}$ relative to baseline ROLES. These tests do not eliminate divergence in all settings, but they support the hypothesis that early-round feedback memory is an important contributor to amplification.

Scope and robustness

Main-text results focus on temperature $T = 0$ to isolate structural effects from sampling-temperature variation. Complementary analyses in SI show that the role-induced instability signature persists across a wider temperature range, consistent with a structural rather than purely thermal interpretation. In other words, setting $T = 0$ does not remove instability; it only removes one explicit noise control while the protocol can still amplify residual variation. Our usage of “chaotic dynamics” is empirical: $\hat{\lambda}$ is estimated from inter-replicate divergence and should be interpreted as an annealed instability index for black-box committee dynamics [Eckmann and Ruelle, 1985, Ott, 2002].

Discussion

The main empirical contribution is a causal decomposition of multi-LLM instability into two experimentally manipulable routes, plus evidence that their interaction is non-additive. For governance, this means committee architecture must be audited as a joint design system rather than tuned along a single “diversity” axis. Importantly, this is an amplification story rather than a zero-to-chaos switch: even baseline uniform/no-role committees can exhibit measurable instability [Selbst et al., 2019, Raji et al., 2020, National Institute of Standards and Technology, 2023, OECD, 2019]. From a deployment perspective, this creates three linked risks: *unpredictability* (replicate-sensitive outcomes), *limited controllability* (small protocol or execution perturbations can redirect the committee to different decision basins), and *limited explainability* (single-run rationales are insufficient summaries of system behavior across replicates).

A second contribution is actionable mechanism. Chair-focused ablation and memory-window interventions suggest that instability can be reduced without collapsing deliberation to a trivial one-step vote. This creates a concrete path from diagnosis to controllable protocol design.

These findings should be interpreted within scope. We do not claim that all multi-LLM committees are chaotic under all tasks. We claim that in the tested protocol family and benchmark, instability is reliably inducible by specific architectural choices and measurably reducible by targeted interventions.

Two next steps are especially important for top-tier review: linking instability to external task quality (accuracy/calibration/decision harm), and extending intervention success criteria from “lower $\hat{\lambda}$ ” to “lower $\hat{\lambda}$ with preserved decision quality.” The present manuscript establishes the stability map needed to run those consequential tests.

Data S1: JSONL run artifacts
Code S1: Experiment and analysis scripts

Materials and Methods

Protocol. We use a windowed-summary deliberation protocol. Each agent receives the scenario prompt, a sliding transcript window (default $k = 15$), and a committee state table; it returns argument text and a structured state line. A deterministic parser extracts preference vectors. One auto-repair pass is allowed on parse failure.

Scenarios. The benchmark contains 12 policy scenarios across immigration, health, income, climate, speech, and AI governance (two scenarios per domain).

Models and conditions. Uniform runs use GPT-4.1-mini. Mixed-model runs use a harmonized one-Grok lineup: Chair (GPT-4.1), Welfare (Claude Sonnet 4.6), Rights (Gemini 2.5 Flash), Equity (Grok-3-mini), Security (GPT-4.1-mini). Core benchmark conditions are NOROLES/ROLES crossed with uniform/mixed model composition at $T = 0$. Additional runs cover role ablation and memory-window variants ($k = 3$, $k = 1$).

Inference and uncertainty. For each condition, we estimate $\hat{\lambda}$ from log-linear fits of $D(t)$ over rounds 3–20. Bootstrap confidence intervals are computed by replicate resampling. Realized n is reported at panel/cell level where relevant. Reporting follows reproducibility-oriented practice for empirical ML benchmarks [Pineau et al., 2021].

Implementation. Experiments and analyses are implemented in Python 3.11 with NumPy, SciPy, and Matplotlib [Virtanen et al., 2020, Hunter, 2007].

Acknowledgments

We thank colleagues for feedback on early drafts and experimental design.

Supplementary Materials

Supplementary Text S1–S3
Supplementary Figures S1–S7
Supplementary Tables S1–S8

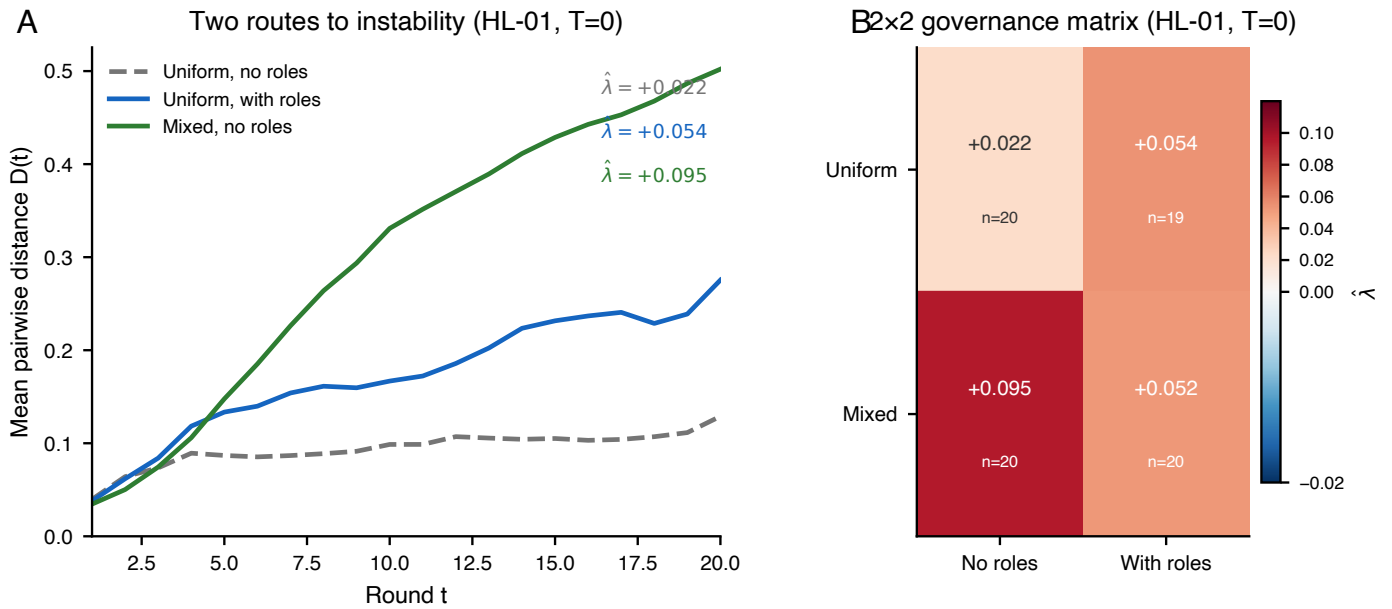


Figure 1: Two design routes to instability and their interaction (HL-01, $T = 0$). (A) Mean pairwise trajectory distance $D(t)$ for three conditions: uniform NOROLES (positive but lower-divergence baseline), uniform ROLES (Route A), and mixed NOROLES (Route B). Both Route A and Route B further amplify divergence. (B) 2×2 matrix crossing roles and model composition. The mixed+roles cell is less unstable than mixed+no-role, showing non-additive interaction. Realized sample sizes are shown in-cell (uniform+roles has slight attrition at $n = 19$; all other cells are $n = 20$).

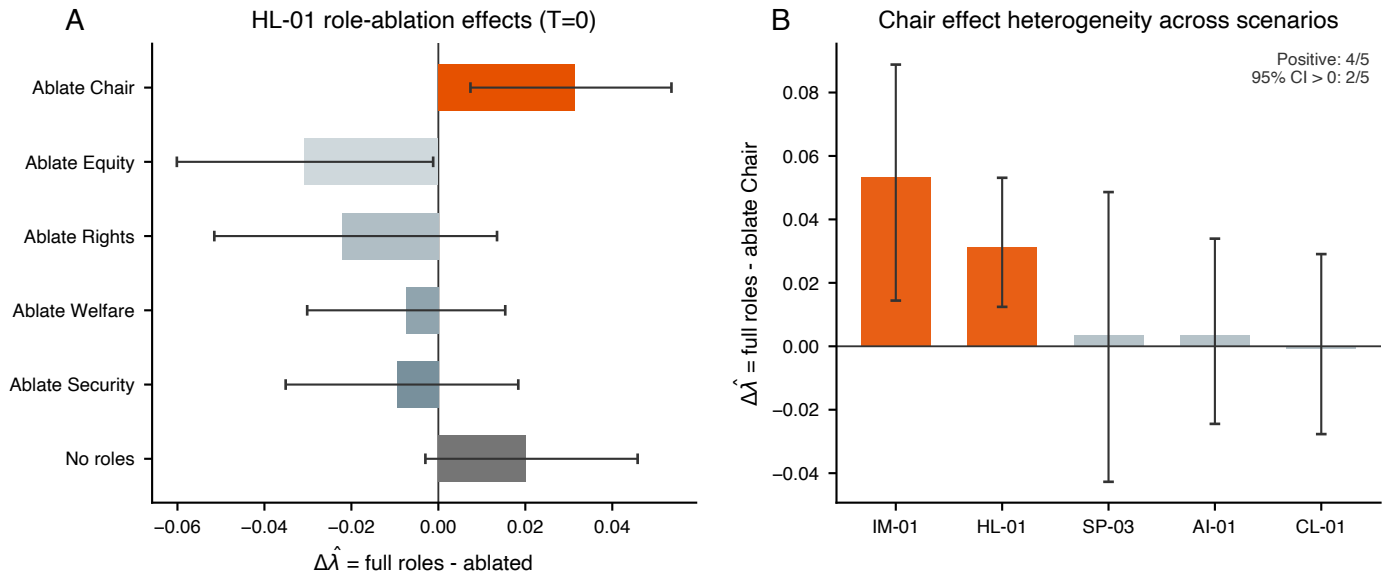


Figure 2: Chair mechanism in HL-01 and cross-scenario heterogeneity. (A) HL-01 role-ablation effects on $\Delta \hat{\lambda} = \hat{\lambda}_{\text{full roles}} - \hat{\lambda}_{\text{ablated}}$. Chair ablation yields the largest reduction among role mandates (with a no-role reference bar shown for context). (B) Scenario-level Chair effect across IM-01, HL-01, CL-01, SP-03, and AI-01, reported as $\Delta \hat{\lambda} = \hat{\lambda}_{\text{full roles}} - \hat{\lambda}_{\text{ablate Chair}}$. Point estimates are positive in all five scenarios, with strongest and best-resolved effects in IM-01 and HL-01.

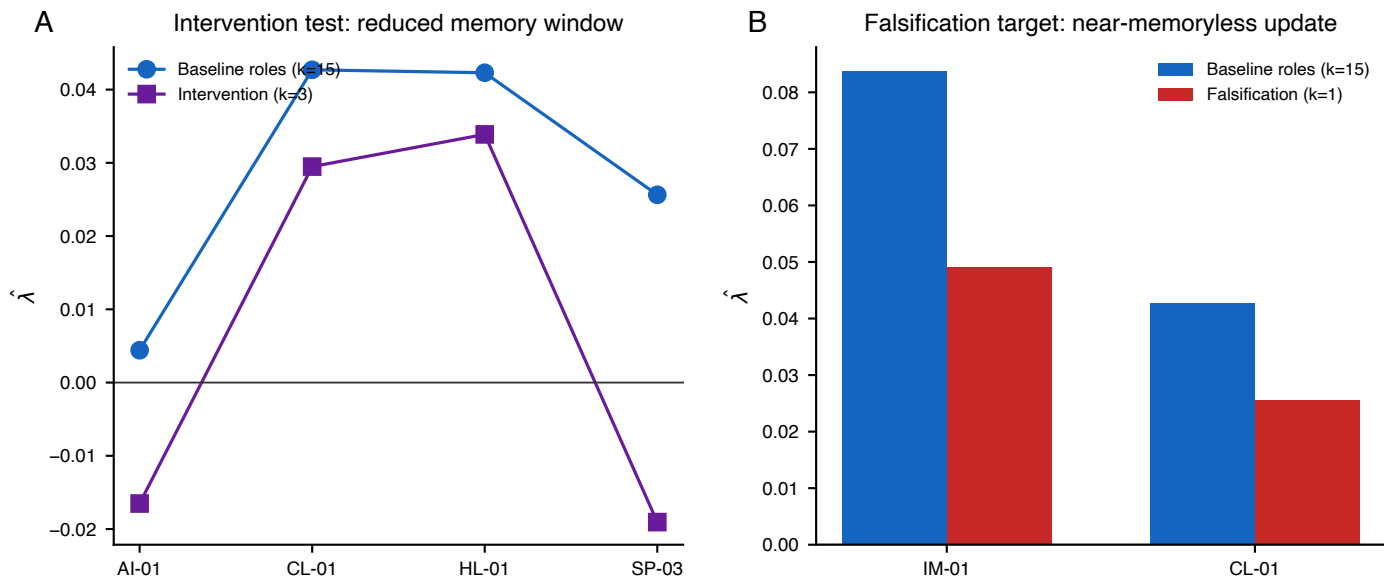


Figure 3: Protocol intervention and falsification tests via memory-depth control. (A) Intervention: reducing memory window from $k = 15$ to $k = 3$ attenuates divergence across four scenarios. (B) Falsification target: collapsing memory to $k = 1$ lowers $\hat{\lambda}$ in IM-01 and CL-01 relative to baseline ROLES. Together these tests support a feedback-memory amplification pathway.

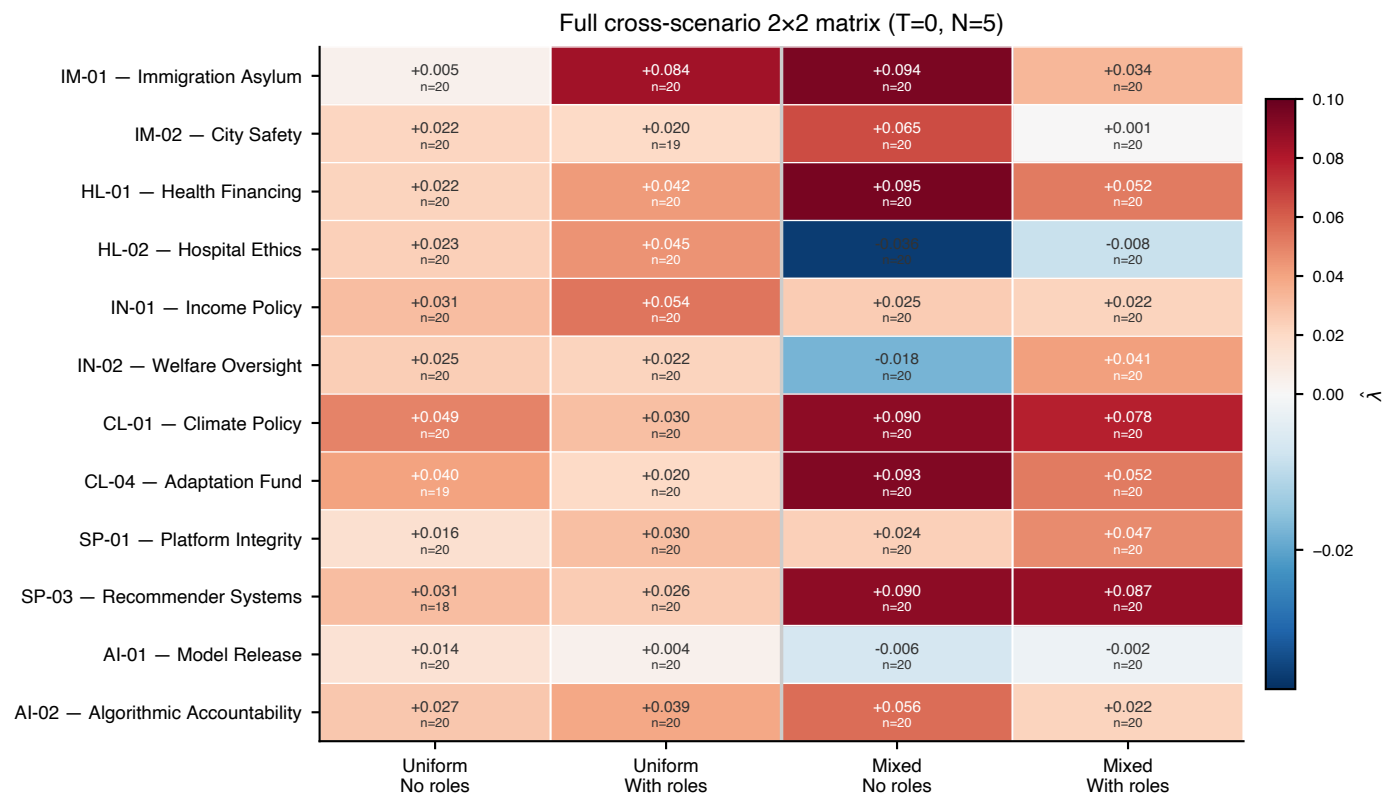


Figure 4: Full cross-scenario 2x2 instability landscape at $T = 0$. Heatmap of $\hat{\lambda}$ across 12 scenarios for uniform/mixed \times no-role/roles conditions. This panel provides the completed benchmark matrix for the two-route claim. Mixed-model cells are all estimated at $n = 20$; uniform cells have realized n displayed in-cell where slight attrition occurred.

References

- Qingyun Wu, Gagan Bansal, Jieyu Zhang, et al. AutoGen: Enabling next-gen LLM applications via multi-agent conversation, 2023. URL <https://arxiv.org/abs/2308.08155>.
- Weize Chen, Yusheng Su, Jingwei Zuo, et al. AgentVerse: Facilitating multi-agent collaboration and exploring emergent behaviors in agents, 2023. URL <https://arxiv.org/abs/2308.10848>.
- Guohao Li, Hasan Hammoud, Hani Itani, Dmitrii Khizbullin, and Bernard Ghanem. CAMEL: Communicative agents for mind exploration of large language model society, 2023. URL <https://arxiv.org/abs/2303.17760>.
- Sirui Hong, Ming Zhuge, Junjie Chen, et al. MetaGPT: Meta programming for multi-agent collaborative framework, 2023. URL <https://arxiv.org/abs/2308.00352>.
- Joon Sung Park, Joseph C. O'Brien, Carrie J. Cai, Meredith Ringel Morris, Percy Liang, and Michael S. Bernstein. Generative agents: Interactive simulacra of human behavior. In *Proceedings of the 36th Annual ACM Symposium on User Interface Software and Technology (UIST)*, pages 1–22, 2023. doi: 10.1145/3586183.3606763.
- Odd Erik Gundersen and Sigbjørn Kjensmo. State of the art: Reproducibility in artificial intelligence. In *Proceedings of the Thirty-Second AAAI Conference on Artificial Intelligence (AAAI)*, pages 1644–1651, 2018.
- Joelle Pineau, Philippe Vincent-Lamarre, Koustuv Sinha, Vincent Larivière, Alina Beygelzimer, Florence d'Alché Buc, Emily Fox, and Hugo Larochelle. Improving reproducibility in machine learning research: A report from the neurips 2019 reproducibility program. *Journal of Machine Learning Research*, 22(164):1–20, 2021. URL <https://jmlr.org/papers/v22/20-303.html>.
- Melanie Sclar, Yejin Choi, Yulia Tsvetkov, and Alane Suhr. Quantifying language models' sensitivity to spurious features in prompt design or: How i learned to start worrying about prompt formatting. In *International Conference on Learning Representations (ICLR)*, 2024. URL <https://arxiv.org/abs/2310.11324>.
- Lianmin Zheng, Wei-Lin Chiang, Ying Sheng, et al. Judging LLM-as-a-Judge with MT-Bench and chatbot arena. In *Advances in Neural Information Processing Systems (NeurIPS)*, volume 36, 2023. URL <https://arxiv.org/abs/2306.05685>.
- Cass R. Sunstein. The law of group polarization. *The Journal of Political Philosophy*, 10:175–195, 2002. doi: 10.1111/1467-9760.00148.
- Amos Tversky and Daniel Kahneman. The framing of decisions and the psychology of choice. *Science*, 211(4481):453–458, 1981. doi: 10.1126/science.7455683.
- Scott E. Page. *The Difference: How the Power of Diversity Creates Better Groups, Firms, Schools, and Societies*. Princeton University Press, 2007.
- Natalie Shapira, Chris Wendler, Avery Yen, Gabriele Sarti, Koyena Pal, Olivia Floody, Adam Belfki, Alex Loftus, et al. Agents of chaos, 2026. URL <https://arxiv.org/abs/2602.20021>.
- Ludwig Arnold. *Random Dynamical Systems*. Springer, Berlin, 1998.
- Lu Hong and Scott E. Page. Groups of diverse problem solvers can outperform groups of high-ability problem solvers. *Proceedings of the National Academy of Sciences*, 101(46):16385–16389, 2004. doi: 10.1073/pnas.0403723101.
- Norbert L. Kerr and R. Scott Tindale. Group performance and decision making. *Annual Review of Psychology*, 55:623–655, 2004. doi: 10.1146/annurev.psych.55.090902.142009.
- Jean-Pierre Eckmann and David Ruelle. Ergodic theory of chaos and strange attractors. *Reviews of Modern Physics*, 57(3):617–656, 1985. doi: 10.1103/RevModPhys.57.617.
- Edward Ott. *Chaos in Dynamical Systems*. Cambridge University Press, 2nd edition, 2002.
- Andrew D. Selbst, Danah Boyd, Sorelle A. Friedler, Suresh Venkatasubramanian, and Janet Vertesi. Fairness and abstraction in sociotechnical systems. In *Proceedings of the Conference on Fairness, Accountability, and Transparency (FAccT)*, pages 59–68, 2019. doi: 10.1145/3287560.3287598.
- Inioluwa Deborah Raji, Andrew Smart, Rebecca N. White, et al. Closing the ai accountability gap: Defining an end-to-end framework for internal algorithmic auditing. In *Proceedings of the Conference on Fairness, Accountability, and Transparency (FAccT)*, pages 33–44, 2020. doi: 10.1145/3351095.3372873.
- National Institute of Standards and Technology. Artificial intelligence risk management framework (AI RMF 1.0). <https://www.nist.gov/itl/ai-risk-management-framework>, 2023. NIST AI 100-1.
- OECD. OECD principles on artificial intelligence. <https://oecd.ai/en/ai-principles>, 2019.
- Pauli Virtanen, Ralf Gommers, Travis E. Oliphant, et al. SciPy 1.0: Fundamental algorithms for scientific computing in Python. *Nature Methods*, 17:261–272, 2020. doi: 10.1038/s41592-020-0772-5.
- J. D. Hunter. Matplotlib: A 2d graphics environment. *Computing in Science & Engineering*, 9(3):90–95, 2007. doi: 10.1109/MCSE.2007.55.

Supplementary Information

Chaotic Dynamics in Multi-LLM Deliberation

Hajime Shimao^{1,*}, Warut Khern-am-nuai², Sung Joo Kim³

¹The Pennsylvania State University, Malvern, PA, USA

²McGill University, Montreal, QC, Canada

³American University, Washington, DC, USA

*Corresponding author: hjs5825@psu.edu

Contents

S1 Server-side Non-Determinism at Temperature Zero	1
S2 Deliberation Protocol and Prompt Templates	2
S2.1 Windowed-Summary (WS) Protocol	2
S2.2 System Prompt Template	2
S2.3 STATE Parsing and Repair	3
S2.4 Clerk Aggregation	3
S2.5 Ablation Protocol	4
S3 Branching Entropy Certificate	4
S3.1 Definition	4
S3.2 Results	4
S4 Semantic Perturbation Analysis	4
S4.1 Rationale	4
S4.2 Variant Construction	5
S4.3 Results	5
S5 Reproducibility and Run Accounting	5
S5.1 Run accounting	5
S5.2 File manifest for reported headline effects	5
S5.3 Failure-source visibility	5

S1 Server-side Non-Determinism at Temperature Zero

Modern LLM APIs document temperature $T = 0$ as producing “deterministic” outputs. In practice, however, cloud-hosted inference involves floating-point arithmetic across heterogeneous GPU clusters, and the result of individual operations is not guaranteed to be bitwise identical across calls. We verified this empirically for OpenAI’s API (model: `gpt-4.1-mini`).

Protocol. We submitted the same prompt 20 times with `temperature=0` and recorded the full text response, the parsed preference vector $\mathbf{p} = (p_A, p_B, p_C)$, and the token-level logprob output (when available). Across all 20 calls with identical prompts, we observe non-zero variance in the output text and the parsed preference vectors in $\approx 40\text{--}50\%$ of trials.

Magnitude. The typical pairwise L2 distance between preference vectors at $T = 0$ after 20 rounds is indistinguishable from that at $T = 0.7$: $\hat{\lambda}(T=0) = 0.0838$ vs. $\hat{\lambda}(T=0.7) = 0.0822$ (both `roles=True`, IM-01, $R = 20$ replicates, 95% CIs overlapping; see Fig. S1).

Interpretation. Server-side floating-point non-determinism represents the *minimum* perturbation that any real-world deployment will face. Our system is therefore a chaos amplifier: even this infinitesimally small noise seed is expanded to macroscopic trajectory divergence by deliberative feedback dynamics. Role differentiation is one strong amplifier, but not a strict prerequisite: in selected scenarios (e.g., HL-01), the uniform no-role baseline remains positive in the completed 2×2 matrix. This makes the chaos result *stronger*, not weaker, as a practical concern: a practitioner cannot escape it even by setting $T = 0$.

S2 Deliberation Protocol and Prompt Templates

S2.1 Windowed-Summary (WS) Protocol

Each deliberation consists of $R = 20$ rounds. At each round, every agent i (in a fixed random order) is called once. The agent receives a context window comprising:

1. The fixed **system prompt** (role mandate + output format instructions).
2. The fixed **scenario packet** (scenario set listed in Supplementary Table S1).
3. The **sliding window** of the last $k = 15$ arguments from the transcript (all agents, chronological), prefixed with role labels.
4. The current **committee state table**: last known parsed state vector $(p_A, p_B, p_C, \text{conf}, \text{tags})$ for each role, presented as a formatted table.

S2.2 System Prompt Template

The system prompt has two parts: a shared preamble and a role-specific mandate.

Shared preamble (all agents):

You are an AI agent participating in a structured committee deliberation. Your committee must reach a collective decision on a policy scenario. You will argue for your position, update it based on evidence and dialogue, and ultimately cast a private ballot.

In every reply you MUST include exactly one STATE line formatted as: `STATE: pref=[pA,pB,pC]; conf=NN; tags=["tag1","tag2"]`

where $p_A+p_B+p_C=1.0$ (floats), `conf` is your confidence (0-100), and `tags` is a list of exactly 2 short concept tags.

Your argument must be at most 110 words. Be direct and specific.

Role mandate (Chair):

ROLE: Chair Your mandate: Facilitate productive deliberation. Synthesize diverse viewpoints, identify points of agreement and disagreement, and help the committee

move toward a reasoned consensus. You may challenge arguments that seem weakly supported. You do not advocate for a predetermined outcome.

Role mandate (Welfare):

ROLE: Welfare Your mandate: Prioritize aggregate welfare, efficiency, and cost-benefit logic. Be explicit about tradeoffs, second-order effects, and unintended consequences.

Role mandate (Rights):

ROLE: Rights Your mandate: Defend individual rights, due process, and non-discrimination. Flag any option that compromises fundamental rights even if it produces aggregate benefits. Deontological constraints take priority.

Role mandate (Equity):

ROLE: Equity Your mandate: Evaluate options through the lens of distributive justice and structural inequality. Flag disparate impacts on historically marginalized groups. Advocate for options that reduce systemic disadvantage.

Role mandate (Security):

ROLE: Security Your mandate: Assess risks to institutional stability, public safety, and long-term systemic resilience. Flag options that introduce unpredictable second-order harms. Prioritize precaution when uncertainty is high.

S2.3 STATE Parsing and Repair

After each agent response, a deterministic regex parser extracts the STATE line:

```
STATE: pref=\[[([0-9. , ]+)\]; conf=([0-9]+); tags=\[[([^\]]*)\]
```

If parsing fails (malformed STATE), a single repair prompt is sent:

```
Your previous response did not contain a valid STATE line. Please respond with ONLY the corrected STATE line in the format: STATE: pref=[pA,pB,pC]; conf=NN; tags=["tag1","tag2"]
```

If parsing still fails after the repair attempt, the run is flagged and excluded from analysis. Across all conditions, the parse-failure rate is below 2%.

Implementation note. In the current codebase, the parser enforces a stricter realization of this template: exactly two tags in snake_case and decimal-formatted preferences.

S2.4 Clerk Aggregation

After all agents complete round R , each agent is called individually for a *private ballot*: a single API call requesting only a JSON object {"decision": "A"|"B"|"C", "confidence": N}. A separate *clerk* agent then receives all private ballots and produces the final committee decision by majority vote:

```
CLERK: You are the vote aggregator. Given the following private ballots [list of ballots], determine the majority decision and return ONLY valid JSON: {"decision": "A"|"B"|"C", "majority_count": N, "total": N}
```

S2.5 Ablation Protocol

For ablation experiments (role-ablation effects in Fig. 2A; full role-ablation panel in Table S5), the ablated role’s mandate is replaced with an empty string. The agent is still present, receives the same transcript window, and must still output a STATE line, but has no specialized framing. This preserves group size $N = 5$ while removing the role’s directional influence.

S3 Branching Entropy Certificate

S3.1 Definition

The branching entropy $\hat{\Gamma}$ quantifies local divergence: from a fixed committee state x_t at round t , we sample $K = 30$ independent continuations of the deliberation and measure how much these trajectories diverge from one another.

Formally, let $\{x_t^{(k)}\}_{k=1}^K$ be K independent continuations from the same initial state x_t . Define:

$$\hat{H}_K = \frac{1}{R-t} \sum_{s=t+1}^R D(\{x_s^{(k)}\}), \quad (1)$$

$$\hat{\mu}(D) = \text{mean pairwise } L_2 \text{ distance among } \{x_t^{(k)}\}, \quad (2)$$

$$\hat{\Gamma} = \hat{H}_K - \hat{\mu}(D), \quad (3)$$

where $D(\cdot)$ is the mean pairwise L2 distance (Eq. 1 of main text). A positive $\hat{\Gamma} > 0$ certifies that the system continues to diverge beyond what is attributable to the initial variation at x_t .

We further compute:

$$\hat{c}_{\text{in}} = \text{mean cosine similarity within each branch cluster}, \quad \hat{c}_{\text{out}} = \text{mean cosine similarity across branch clusters}. \quad (4)$$

A chaotic system should show $\hat{c}_{\text{in}} > \hat{c}_{\text{out}}$: trajectories within a branch resemble each other more than trajectories across branches.

S3.2 Results

We ran $K = 30$ continuations from 5 independently chosen base states (replicates 0–4) for IM-01 at $T = 0.7$, roles=True. Results are shown in Fig. S6. Across all 5 replicates:

- $\hat{\Gamma} = 0.054 \pm 0.008 \text{ SE} > 0$ (all replicates individually positive).
- $\hat{c}_{\text{in}} > \hat{c}_{\text{out}}$ in all 5 replicates.

These results confirm that the system has a rich local attractor landscape: small perturbations from the same state produce qualitatively different downstream trajectories.

S4 Semantic Perturbation Analysis

S4.1 Rationale

The main text shows that server-side FP noise (temperature $T = 0$, identical prompts) is sufficient to drive $\hat{\lambda} > 0$. A separate question is whether changes in surface wording—keeping the semantic content

of the scenario identical—produce additional divergence. This matters for practical governance: if a policy scenario phrased slightly differently by two different civil servants leads to qualitatively different AI committee decisions, the decisions are not semantically auditable.

S4.2 Variant Construction

We constructed 6 phrasings of the IM-01 immigration scenario:

1. **Canonical** — the original scenario text.
2. **Formal register** — bureaucratic vocabulary, passive voice.
3. **Conversational** — plain-English rephrasing, active voice, simplified numbers.
4. **Legalistic** — statutory citation style, conditional clauses.
5. **Passive reframe** — all active policy frames restated as passive constraints (“grants may be allocated” vs. “allocate grants”).
6. **Synonym swap** — systematic substitution of key nouns and verbs with near-synonyms (e.g., “applicant” → “petitioner”, “allocate” → “distribute”).

Semantic equivalence was verified by having GPT-4o score each variant pair on a 0–10 meaning-preservation scale; all pairs scored ≥ 8.5 .

S4.3 Results

Each variant was run once at $T = 0$ with `roles=True` for 20 rounds. The 6 trajectories are shown in Fig. S7. The empirical Lyapunov exponent across the 6 variants is $\hat{\lambda} = 0.030$ (compared to $\hat{\lambda} = 0.0838$ for 20 replicates of the canonical phrasing with FP noise).

Two variants (*Passive reframe* and *Conversational*) converge to option B, while the remaining four converge to option A. With only six variants, this split should be interpreted as directional rather than definitive. The smaller $\hat{\lambda}$ compared to the FP-noise condition (0.030 vs. 0.084) reflects that synonym-level perturbations are smaller than server-side FP noise in this system—but still non-zero, confirming that surface wording affects collective decisions even when semantic content is preserved.

S5 Reproducibility and Run Accounting

S5.1 Run accounting

Table S1 reports target versus realized replicate counts for key conditions used in the main narrative (including the HL-01 headline 2×2 panel and IM-01 mechanism/temperature panels).

S5.2 File manifest for reported headline effects

Table S2 maps headline results to exact JSONL files used for analysis and plotting.

S5.3 Failure-source visibility

Current JSONL artifacts store successful runs only. As a result, unresolved replicate deficits can be quantified, but failure *type* (parser failure vs. provider timeout/quota vs. interruption) is not fully

recoverable for all historical runs. Table S3 documents this limitation.

Table S1: Run accounting for key reported conditions. Target and realized replicate counts as of March 10, 2026. Deficit = target minus realized.

Group	Condition	Target	Realized	Deficit
Headline	HL-01: Uniform no-role ($T = 0$)	20	20	0
Headline	HL-01: Uniform roles ($T = 0$)	20	19	1
Headline	HL-01: Mixed no-role ($T = 0$)	20	20	0
Headline	HL-01: Mixed roles ($T = 0$)	20	20	0
Core	Uniform no-role (IM-01, $T = 0$)	20	20	0
Core	Uniform roles (IM-01, $T = 0$)	20	20	0
Core	Mixed no-role (IM-01, $T = 0$)	20	20	0
Core	Mixed roles (IM-01, $T = 0$)	20	20	0
Core	12-scenario matrix: Uniform no-role total	240	237	3
Core	12-scenario matrix: Uniform roles total	240	236	4
Core	12-scenario matrix: Mixed no-role total	240	240	0
Core	12-scenario matrix: Mixed roles total	240	240	0
Ablation	Ablate Chair (IM-01, $T = 0$)	20	20	0
Ablation	Ablate Equity (IM-01, $T = 0$)	20	20	0
Semantics	6 IM-01 semantic variants	6	6	0
Provider	GPT-4.1, roles=True, $T = 0$	20	20	0
Provider	Claude Sonnet 4.6, roles=True, $T = 0$	20	19	1
Provider	Gemini 2.5 Flash, roles=True, $T = 0$	20	20	0
Provider	Grok-3, roles=True, $T = 0$	20	16	4

Table S2: File manifest for headline reported effects. Paths are relative to project root. Mixed-model matrix files are read from synced VM shards in `data/vm_sync/.../chaos_v1_one_grok_t0_matrix/` (with fallback to local archived copies).

Effect	JSONL file
HL-01 uniform no-role baseline (Fig. 1)	<code>data/raw/chaos_v1/HL-01__T0.0__N5__rolesFalse.jsonl</code>
HL-01 uniform role effect (Fig. 1)	<code>data/raw/chaos_v1/HL-01__T0.0__N5__rolesTrue.jsonl</code>
HL-01 mixed no-role route (Fig. 1)	<code>data/vm_sync/.../chaos_v1_one_grok_t0_matrix/HL-01__T0.0__N5__ro</code>
HL-01 mixed+roles interaction (Fig. 1)	<code>data/vm_sync/.../chaos_v1_one_grok_t0_matrix/HL-01__T0.0__N5__ro</code>
IM-01 uniform no-role baseline	<code>data/raw/chaos_v1/IM-01__T0.0__N5__rolesFalse.jsonl</code>
IM-01 uniform role effect	<code>data/raw/chaos_v1/IM-01__T0.0__N5__rolesTrue.jsonl</code>
IM-01 mixed no-role route	<code>data/raw/chaos_v1/IM-01__T0.0__N5__rolesFalse__multimodel.jsonl</code>
IM-01 mixed+roles interaction	<code>data/raw/chaos_v1/IM-01__T0.0__N5__rolesTrue__multimodel.jsonl</code>
Full 12-scenario mixed matrix	<code>data/vm_sync/.../chaos_v1_one_grok_t0_matrix/{scenario}__T0.0__N</code>
Chair ablation	<code>data/raw/chaos_v1/IM-01__T0.0__N5__rolesTrue__ablate-Chair.jsonl</code>
Chair replication panel	<code>data/vm_sync/instance-20260307-022228/chaos_v1_chair_rep_t0/*.js</code>
Intervention (k=3) panel	<code>data/vm_sync/instance-20260307-022228/chaos_v1_intervention_kw3</code>
Falsification (k=1) panel	<code>data/vm_sync/instance-20260307-022228/chaos_v1_falsification_kw1</code>
Temperature robustness (ROLES, $T = 0.7$)	<code>data/raw/chaos_v1/IM-01__T0.7__N5__rolesTrue.jsonl</code>
Temperature robustness (NOROLES, $T = 0.7$)	<code>data/raw/chaos_v1/IM-01__T0.7__N5__rolesFalse.jsonl</code>
Semantic perturbation	<code>data/raw/semantic_v1/IM-01__T0.0__N5__rolesTrue.jsonl</code>

Table S3: Failure-source visibility in current artifacts. “Known” means directly inferable from stored artifacts; “Unknown” means not reconstructable without external runtime logs.

Failure source	Status	Notes
Provider timeout / quota / API errors	Partially known	Seen indirectly via realized $n < \text{target}$ in provider rows.
Parser failure after repair	Unknown	Successful JSONL files do not persist parser-failure counters.
Manual interruption / VM stop	Unknown	Requires external process logs, not bundled in Data S1.

Supplementary Figures

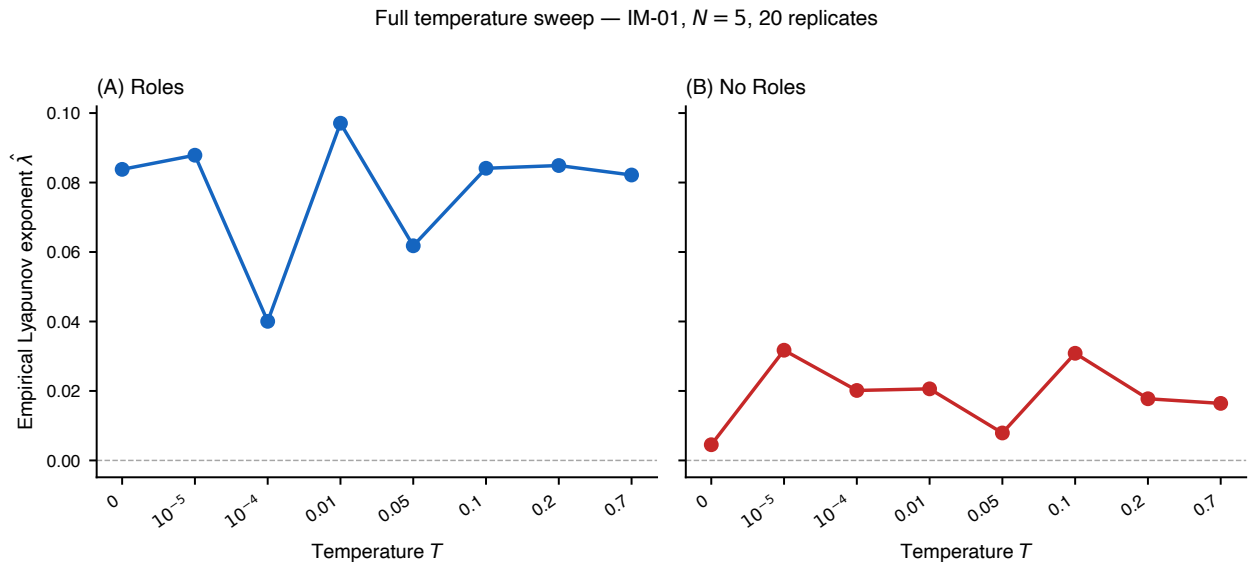


Figure S1: Full temperature sweep for both role conditions. Empirical Lyapunov exponent $\hat{\lambda}$ as a function of temperature $T \in \{0, 10^{-5}, 10^{-4}, 0.01, 0.05, 0.1, 0.2, 0.7\}$ for **(A)** ROLES and **(B)** NO ROLES deliberation (IM-01, $N = 5$, 20 replicates each). Under ROLES, $\hat{\lambda}$ is statistically flat across all eight conditions. Under NO ROLES, $\hat{\lambda}$ is uniformly suppressed and statistically indistinguishable from zero in seven of eight conditions. Shaded bands: 95% bootstrap CI (500 resamples).

Per-agent preferences (p_A solid, p_B dashed) — IM-01, $T = 0$, roles=True; 6 representative runs

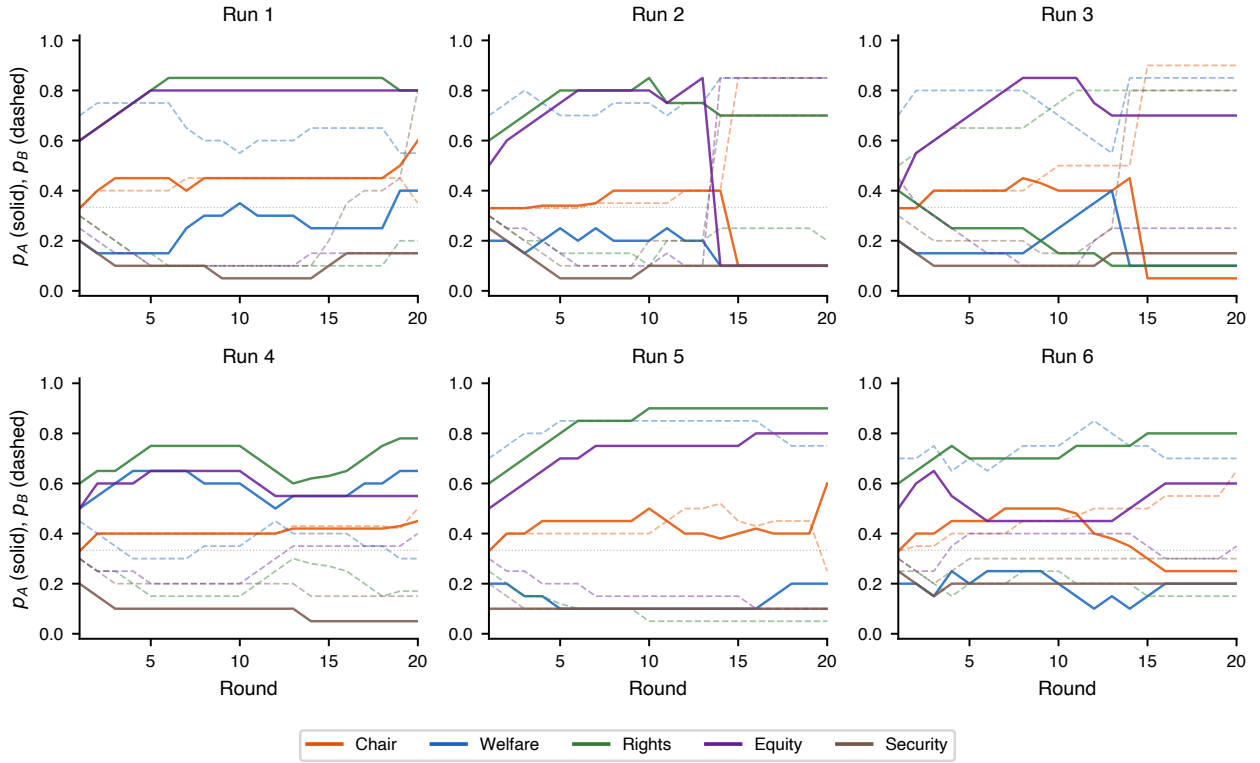


Figure S2: Per-agent preference trajectories across 6 representative runs. Solid lines show p_A (preference for option A) and dashed lines show p_B (preference for option B) for each of the five agents, color-coded by role (Chair: orange; Welfare: blue; Rights: green; Equity: purple; Security: brown). The Chair (orange) exhibits the most dynamic switching behavior, while Rights (green) and Security (brown) tend toward stable preferences. Condition: IM-01, $T = 0$, roles=True.

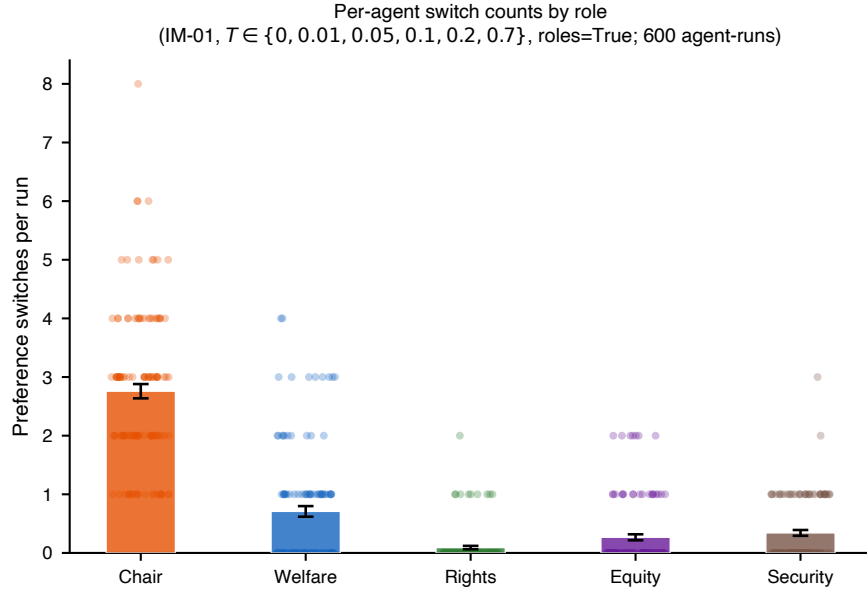


Figure S3: Per-agent preference switch counts by role. Bars show mean \pm SEM switch counts; points show individual agent-run values (jittered). Data pooled across $T \in \{0, 0.01, 0.05, 0.1, 0.2, 0.7\}$, roles=True, IM-01. The Chair is the dominant switching agent (mean ≈ 2.76 switches/run), with all non-Chair roles below one switch/run on average. This asymmetry identifies the Chair as the mechanistic source of chaotic amplification.

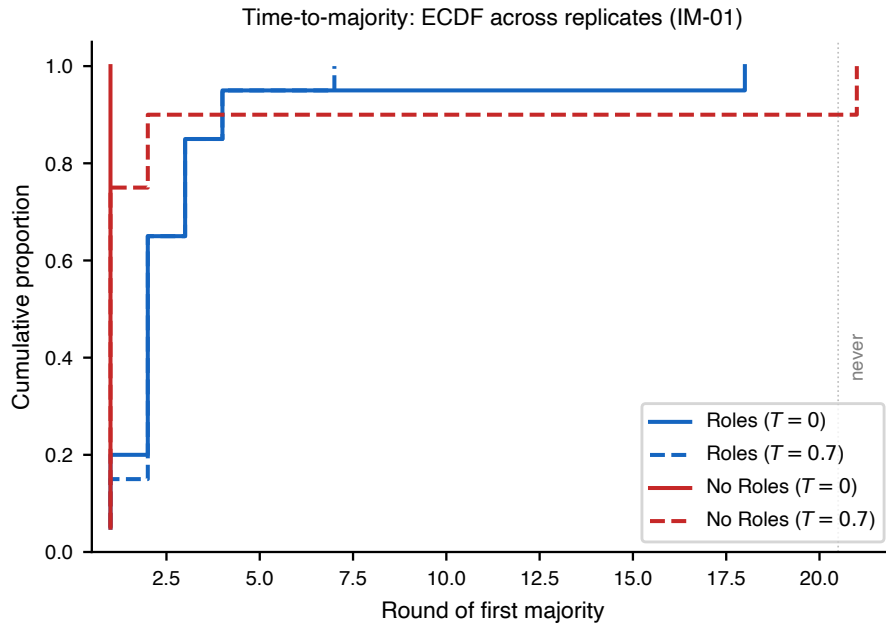


Figure S4: Time-to-majority: empirical CDF across replicates. Each curve shows the fraction of runs in which a strict majority (≥ 3 of 5 agents) first converged on the same top-preference option by a given round, for four conditions on IM-01 (roles \times temperature). Under NOROLES, consensus forms in round 1 without exception. Under ROLES, consensus is delayed to rounds 2–3, with a non-trivial fraction of runs (10–20%) never achieving stable majority within 20 rounds. “Never” ($t > 20$) is plotted at $x = 21$.

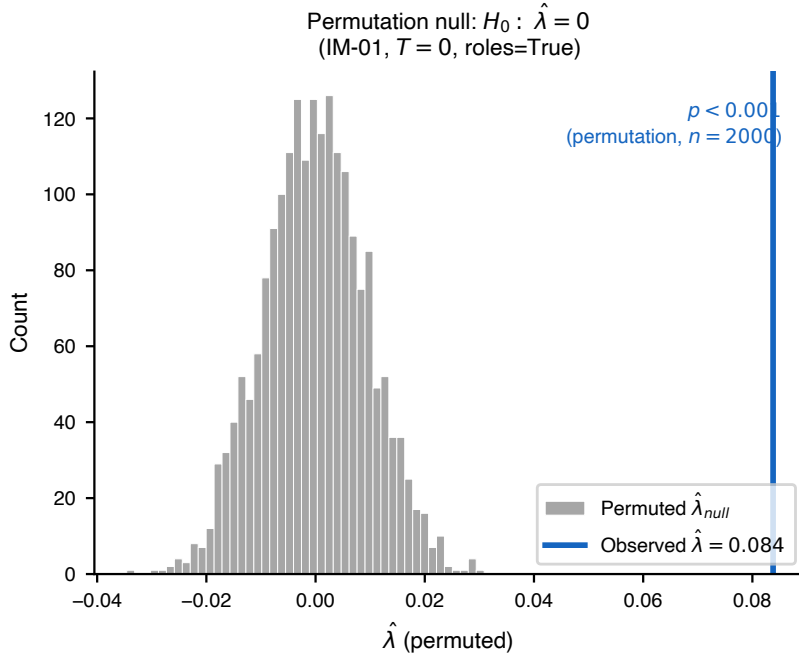


Figure S5: Permutation null test for $H_0: \hat{\lambda} = 0$. Gray histogram: distribution of $\hat{\lambda}_{null}$ from 2,000 permutations (round indices shuffled within each replicate). Vertical blue line: observed $\hat{\lambda}_{obs}$. The observed value lies far in the right tail of the null distribution; $p < 0.001$. Condition: IM-01, $T = 0$, roles=True.

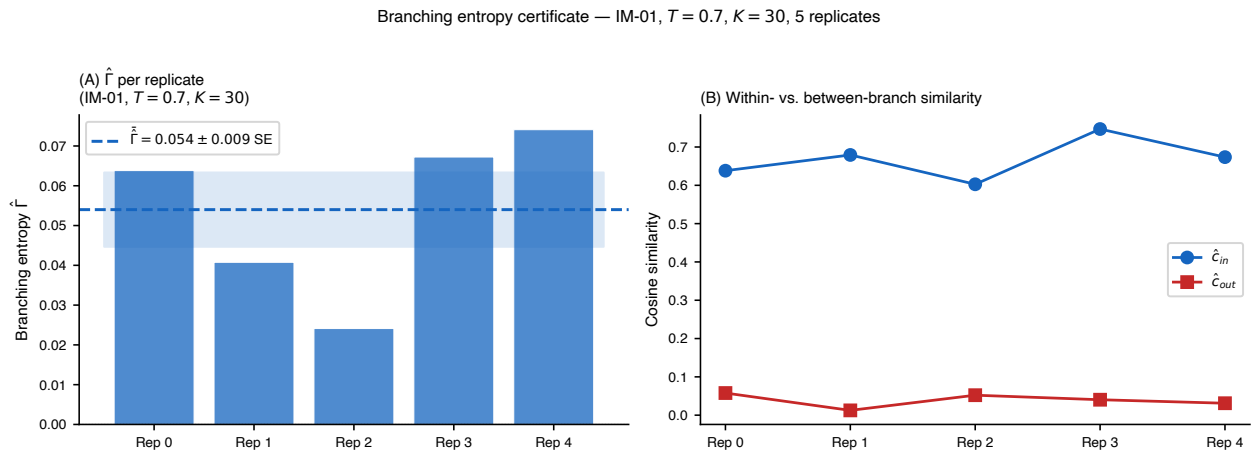


Figure S6: Branching entropy certificate $\hat{\Gamma}$ across replicates. (A) $\hat{\Gamma}$ for each of 5 replicates (IM-01, $T = 0.7$, $K = 30$ independent continuations per replicate). Dashed line: mean $\hat{\Gamma} = 0.054$; shaded band: ± 1 SE. All 5 replicates show $\hat{\Gamma} > 0$, certifying that the system continues to diverge beyond its initial variation. (B) Within-branch (\hat{c}_{in}) vs. between-branch (\hat{c}_{out}) cosine similarity of preference vectors; $\hat{c}_{in} > \hat{c}_{out}$ in all replicates, confirming structured attractor organization.

Semantic perturbation — IM-01, $T = 0$, roles=True
 6 synonym/register rephrasings of the same scenario

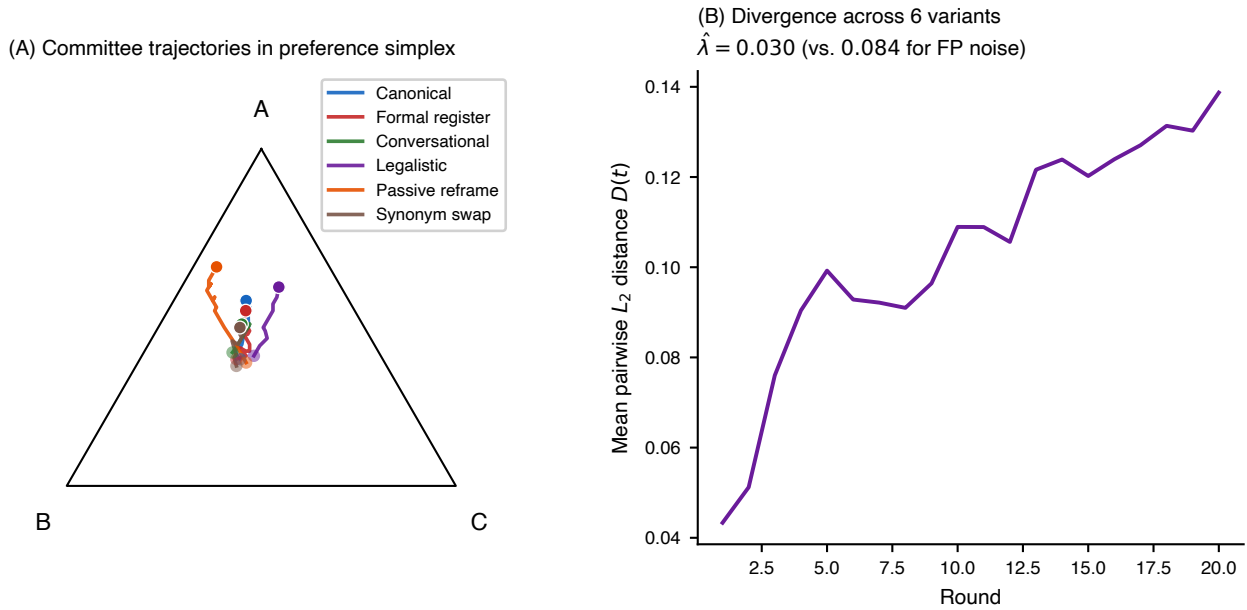


Figure S7: Semantic perturbation: 6 synonym/register rephrasings of IM-01. (A) Committee mean preference trajectories in the simplex for each of the 6 variants at $T = 0$, roles=True. Filled circles indicate final-round positions. Four variants (Canonical, Formal, Legalistic, Synonym swap) converge to option A; two (Passive reframe, Conversational) converge to option B, demonstrating that surface framing affects collective outcomes even when semantic content is preserved (all pairs score $\geq 8.5/10$ on AI-judged meaning preservation). (B) Mean pairwise L2 divergence across the 6 variants ($\hat{\lambda} = 0.030$), smaller than FP-noise divergence ($\hat{\lambda} = 0.0838$) and directionally above zero.

Supplementary Tables

Table S4: All 12 policy scenarios. Each scenario is a structured policy deliberation packet presented to the AI committee verbatim. Options A, B, C are designed to be approximately balanced in social desirability. Full scenario texts are in Data S1.

ID	Domain	Type	Options (A / B / C)	Decision question
IM-01	Immigration	choice_ABC	Humanitarian / Balanced points / Deterrence+verification	Which rule should be used?
IM-02	Immigration	choice_ABC	Full cooperation / Limited cooperation / Non-cooperation	Should city police enforce immigration laws?
HL-01	Health	choice_ABC	Single-payer / Public option / Regulated multi-payer	Which system best balances cost and quality?
HL-02	Health	choice_ABC	Maximize lives / Maximize life-years / Equity lottery	What is the best way to allocate scarce resources?
IN-01	Income	choice_ABC	UBI / Targeted cash transfer / Negative income tax	Is universality worth the cost?
IN-02	Income	choice_ABC	Strict work requirements / Moderate requirements / No requirements	Is conditionality necessary for support?
CL-01	Climate	choice_ABC	Carbon tax+dividend / Cap-and-trade / Sectoral regulations	Is pricing carbon the most effective approach?
CL-04	Climate	allocation	Sea walls / Relocation / Insurance / Heat / Wildfire	Should adaptation be prioritized for equity?
SP-01	Speech	choice_ABC	Remove content / Label+downrank / Minimal intervention	Is harm prevention worth the trade-off in free speech value?
SP-03	Speech	choice_ABC	Keep engagement ranking / Reduce amplification / User-choice	Should platform algorithms be more transparent?
AI-01	AI governance	choice_ABC	Open weights / Licensed release / API-only	Should openness be required for safety?
AI-02	AI governance	choice_ABC	Mandatory audits / Voluntary+incentives / No mandate	Is prevention of misuse more important than innovation?

Table S5: Full empirical Lyapunov exponent table. $\hat{\lambda}$ for all IM-01 conditions used in the main experiments. Flip rate = fraction of runs with non-modal final decision. TTM = median time-to-majority (rounds).

Condition	$\hat{\lambda}$	Flip rate	TTM	n
<i>Temperature sweep (IM-01, N=5, roles=True)</i>				
$T = 0.7$	0.0822	0.400	2	20
$T = 0.2$	0.0849	0.550	2	20
$T = 0.1$	0.0841	0.450	2	20
$T = 0.05$	0.0618	0.450	2	20
$T = 0.01$	0.0971	0.450	2	20
$T = 10^{-4}$	0.0400	0.400	2	20
$T = 10^{-5}$	0.0879	0.500	2	20
$T = 0$ (same prompt)	0.0838	0.450	2	20
<i>Temperature sweep (IM-01, N=5, roles=False)</i>				
$T = 0.7$	0.0164	0.000	1	20
$T = 0.2$	0.0178	0.000	1	20
$T = 0.1$	0.0308	0.050	1	20
$T = 0.05$	0.0079	0.000	1	20
$T = 0.01$	0.0206	0.000	1	20
$T = 10^{-4}$	0.0201	0.000	1	20
$T = 10^{-5}$	0.0317	0.000	1	20
$T = 0$ (same prompt)	0.0045	0.000	1	20
<i>Semantic perturbation (IM-01, T=0, roles=True, 6 variants)</i>				
Across 6 phrasings	0.0300	0.333	2	6
<i>Role ablation (IM-01, T=0, roles=True, role mandate removed)</i>				
Ablate Chair	0.0304	0.000	16	20
Ablate Welfare	0.0680	0.300	2	20
Ablate Rights	0.0711	0.500	2	20
Ablate Equity	0.0413	0.250	2	20
Ablate Security	0.0822	0.450	2	20
No ablation	0.0838	0.450	2	20

Table S6: Cross-model empirical Lyapunov exponents. $\hat{\lambda}$ for IM-01 at $T \in \{0, 0.1\}$, roles=True and roles=False, for four model families plus the GPT-4.1-mini baseline. Values shown as $\hat{\lambda}$ with run count in parentheses.

Provider	Model	Roles=True		Roles=False	
		$T = 0$	$T = 0.1$	$T = 0$	$T = 0.1$
OpenAI	GPT-4.1	0.0509 (20)	0.0661 (20)	0.0308 (20)	0.0403 (20)
Anthropic	Claude Sonnet 4.6	0.0626 (19)	0.0449 (20)	0.0479 (19)	-0.0079 (19)
Google	Gemini 2.5 Flash	0.1058 (20)	0.1275 (19)	0.0693 (20)	0.0940 (20)
xAI	Grok-3	0.0982 (16)	0.1164 (16)	0.0348 (19)	0.0373 (20)
<i>Baseline (GPT-4.1-mini)</i>		0.0838 (20)	0.0841 (20)	0.0045 (20)	0.0308 (20)

Note: Run counts below 20 reflect provider-timeout or quota attrition during data collection.

Table S7: Per-agent mean preference switch counts by role. Data pooled across $T \in \{0, 0.01, 0.05, 0.1, 0.2, 0.7\}$, roles=True, IM-01. Values are mean \pm SD; n = number of agent-runs.

Role	Mean switches	SD	n
Chair	2.76	1.33	120
Welfare	0.71	0.99	120
Rights	0.09	0.32	120
Equity	0.27	0.56	120
Security	0.34	0.54	120

Table S8: Chaos landscape: $\hat{\lambda}$ for all 12 scenarios. All conditions use $N = 5$ with target 20 replicates per condition. Values shown here are point estimates from the current landscape run files.

Scenario	Roles=True		Roles=False	
	$T = 0$	$T = 0.1$	$T = 0$	$T = 0.1$
IM-01	0.0838	0.0841	0.0045	0.0308
IM-02	0.0202	0.0160	0.0216	0.0190
HL-01	0.0541	0.0495	0.0221	0.0144
HL-02	0.0447	0.0680	0.0235	0.0233
IN-01	0.0536	0.0489	0.0309	0.0245
IN-02	0.0222	0.0218	0.0246	0.0270
CL-01	0.0427	0.0904	0.0493	0.0615
CL-04	0.0199	0.0133	0.0403	0.0336
SP-01	0.0304	0.0651	0.0163	0.0274
SP-03	0.0308	0.0466	0.0311	0.0273
AI-01	0.0032	0.0231	0.0144	0.0350
AI-02	0.0385	0.0573	0.0270	0.0351

Note: Values are from currently available landscape files; realized run counts can vary slightly (see Table S1).